ISBN: 978-3-95450-247-9 ISSN: 2673-5490 doi: 10.18429/JACoW-IPAC2024-THPC06

IMPACT-T SIMULATION FOR THE LATEST COHERENT ELECTRON COOLING POP EXPERIMENT*

K. Shih†, G. Wang, J. Ma, I. Pinayev, Y. Jing,
Brookhaven National Laboratory, Upton NY, USA
V. N. Litvinenko, I. Petrushina, Stony Brook University, Stony Brook NY, USA

Abstract

This paper presents the results of the IMPACT-T [1, 2] simulation conducted for the latest iteration of the Coherent Electron Cooling (CeC) Pop Experiment [3] at Brookhaven National Laboratory (BNL). The CeC experiment aims to demonstrate the principles of CeC, a rapid cooling technique designed for high-energy hadron beams. In addition to presenting simulation results for the current lattice parameters, this paper includes a discussion of the benchmarking results obtained from IMPACT-T simulations and real CeC experiments. These comprehensive simulations not only facilitate the fine-tuning of CeC lattice parameters but also offer insights into the ongoing performance enhancements, all aimed at achieving exceptional beam quality.

INTRODUCTION

For our simulations in the CeC experiment, we utilized Impact-T, a robust, three-dimensional particle-in-cell (PIC) simulation code [4] developed at Lawrence Berkeley National Laboratory. This code is adept at tracking relativistic particles and incorporates effects such as space-charge forces, short-range wakefields, and coherent synchrotron radiation wakefields. Impact-T's method of solving particle self-field interactions through integrated Green's function-based mean-field solvers enhances its effectiveness. It also supports complex beamline structures by allowing the superposition of external-field elements, which can be defined in detailed three-dimensional configurations.

Using the Impact-T code, we successfully conducted a comprehensive simulation of the entire CeC beamline, from start to finish. Our advanced simulation tools have significantly reduced the time required to prepare the high-quality CeC electron beam. In this paper, we present our Impact-T simulation modeling and the benchmarking results that have emerged from our work with the CeC experiment.

THE CeC GUN CAVITY SIMULATION

One of the initial challenges encountered was integrating the relatively lengthy CeC beam into the gun simulation. The high field gradient of our superconducting RF 113 MHz quarter-wave gun cavity [5, 6] induces a significant head-to-tail velocity difference in the CeC electron beam as it traverses the gun cavity. This poses a substantial challenge for PIC simulations that utilize quasi-static approximations [7], which presuppose minor velocity differences within the same beam frame. As a result, space charge calculations were originally confined to a single beam frame, applying the Lorentz transformation based on its average energy. Unfortunately, this approach proved inadequate for the CeC experiment. Figure 1 illustrates the distribution of the longitudinal beta values of the CeC beam within the gun cavity, where the RMS velocity spread of the electron bunch can exceed 20% at certain instances.

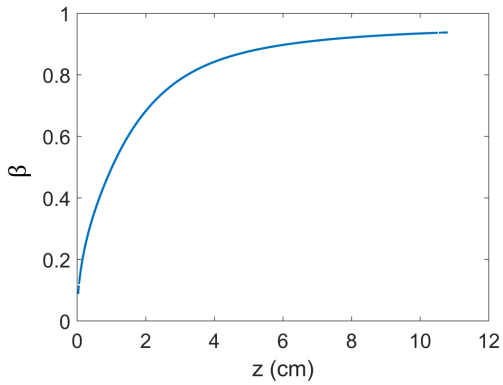

Figure 1: Plotting particle velocities versus longitudinal particle locations of the Impact-T simulated CeC beam while inside the CeC SRF Gun.

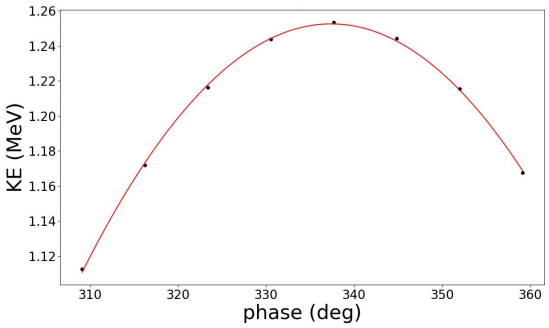

Figure 2: Plot of the CeC electron beam's kinetic energy after the gun cavity as a function of the cavity phase. Black dots represent the simulated data; the red curve is the quadratic fitting.

To address this, the Impact-T simulation of our CeC SRF gun required a unique approach. We divided the CeC electron bunch into four segments just beyond the cathode for the purposes of the simulation. Impact-T processed these segments independently, applying an individual Lorentz transformation to each segment based on its mean velocity. Additionally, the code aggregated the total space-charge forces to

* Work supported by DOE
† kshih@bnl.gov

ISBN: 978-3-95450-247-9 ISSN: 2673-5490 doi: 10.18429/JACoW-IPAC2024-THPC06

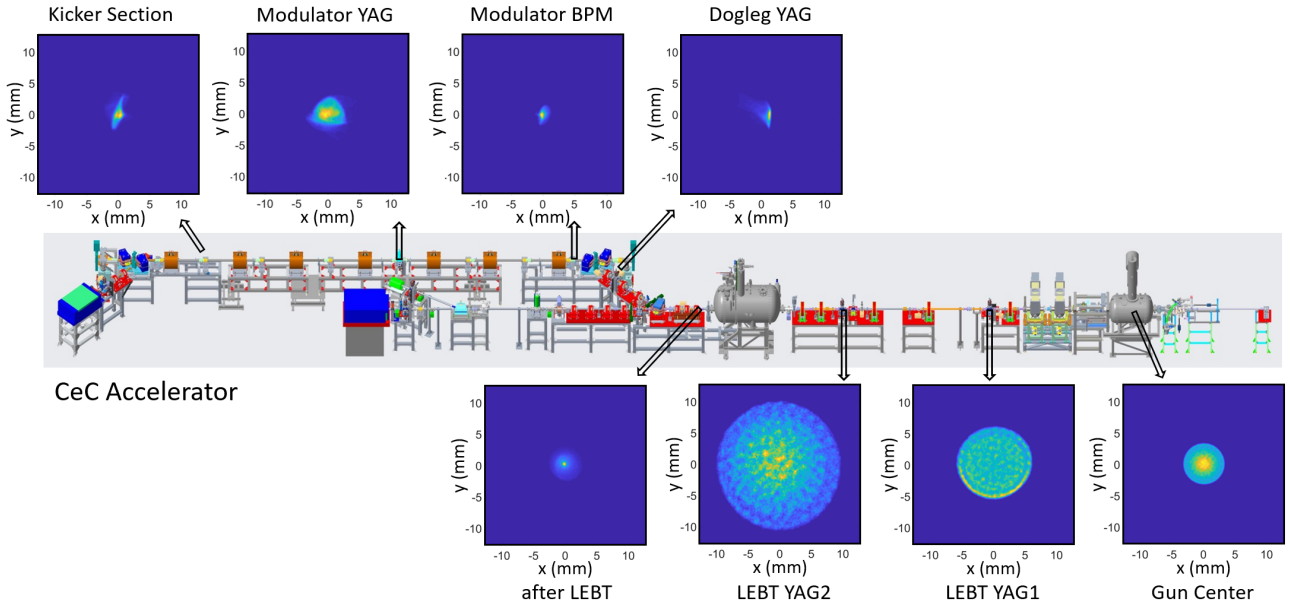

Figure 3: Impact-T simulated transverse beam projection profiles at various locations along the CeC beamline, as indicated by the black arrows on the schematic diagram of the CeC accelerator.

progress the motion of each particle individually. Although increasing the number of bunch segments enhances the accuracy of space-charge calculations, it also linearly increases the simulation duration. Opting for four segments in our bunch segmentation during the CeC SRF Gun simulation represented a balance between simulation time and accuracy. Moreover, further segmentation beyond four slices showed diminishing returns in terms of changes in beam emittance and size.

IMPACT-T SIMULATION DEMONSTRATION

This section presents the comprehensive simulation of the CeC experiment using the Impact-T software. The simulation begins with the generation of a 380 ps long, 1.5 nC electron beam by the photocathode within the SRF gun cavity, which is then initially accelerated to an energy of 1.25 MeV. The electron beam subsequently passes through a bunching cavity [8] to achieve the required peak current for the CeC experiment. All RF cavities within the CeC beamline are calibrated in the Impact-T model to match those used in the actual experiment.

For instance, we adjust the beam energy at a position just beyond the gun cavity by altering the gun phase. Figure 2 illustrates the relationship between the beam kinetic energy and the gun cavity phase during the Impact-T simulation, enabling precise replication of the experimental conditions.

Following its exit from the bunching cavity, the electron beam traverses five LEBT solenoids that provide transverse focusing, before final energy boosting in the CeC linac. Additionally, two YAG profile monitors along this beamline aid in verifying the accuracy of the Impact-T model by comparing it with observed YAG images. The most straightforward verification involves comparing changes in the RMS beam size by adjusting an upstream solenoid. Only then should three-dimensional effects, such as machine misalignment, be incorporated into the simulation.

The CeC Linac, a five-cell superconducting RF (SRF) cavity operating at 704 MHz [9, 10], accelerates the electron beam from a relativistic gamma factor of $\gamma = 3.45$ to $\gamma = 28.50$. This acceleration synchronizes the velocity of the CeC electron beam with that of the RHIC hadron beam in the CeC Interaction section. By utilizing the YAG screen in the subsequent Dogleg section, we confirm that the longitudinal phase space of the Impact-T simulated beam corresponds with experimental observations.

After this section, the CeC electron beam merges with the incoming RHIC beam and passes through the PCA, which consists of periodic solenoid structures. We use the YAG screen presented in this section for further comparisons and fine-tuning of the model. Figure 3 depicts the start-to-end simulation of the CeC accelerator structure. The diagnostic plots shown in Fig. 3 were specifically designed to mimic the function of the YAG screen diagnostic [11], providing an improved basis for comparison with experimental diagnostics.

BENCHMARKING WITH THE CeC EXPERIMENT

The simulation results showcased here stem from one of the latest CeC test run lattice configurations. We have validated these results against the CeC YAG diagnostic measurements, as depicted in Fig. 4. Across the entire CeC beamline, the YAG beam profiles demonstrated a robust correlation with the simulated profiles, both in terms of dimensional accuracy and specific beam characteristics. For example, the

ISBN: 978-3-95450-247-9 ISSN: 2673-5490 doi: 10.18429/JACoW-IPAC2024-THPC06

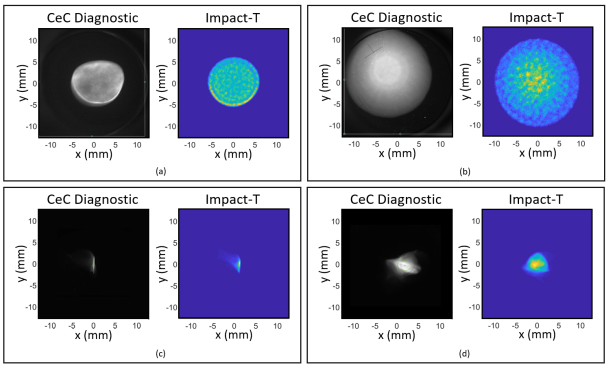

Figure 4: The benchmarking result of the Impact-T start-to-end simulation model. (a) was the beam image comparison at CeC LEBT YAG1. (b) CeC LEBT YAG2. (c) CeC Dogleg YAG. (d) CeC Modulator YAG.

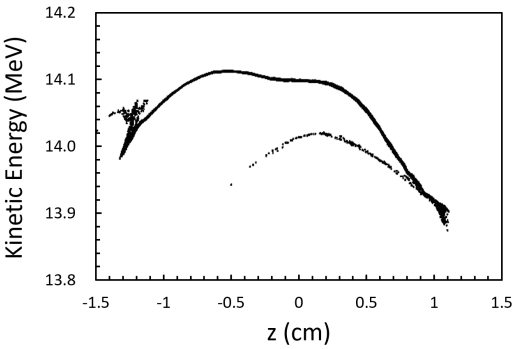

Figure 6: Longitudinal energy phase space of the CeC electron bunch as simulated by the Impact-T start-to-end model. This bunch is depicted in Fig. 5(b) at the CeC Dogleg YAG location.

CeC LEBT YAG1 beam profile, shown in Fig. 4(a), reveals the highest charge density on the lower half of the beam rim, a result of an upstream misaligned gun cavity. The CeC Dogleg YAG and the CeC Modulator YAG comparisons further affirmed the model's accuracy in capturing both alignment and asymmetrical beam projections.

Additionally, we benchmarked the longitudinal beam energy profile in the dispersive region downstream of the first CeC bending dipole. The accuracy of our simulation in the longitudinal energy domain was corroborated through comparisons with the CeC Dogleg YAG images, as shown in Fig. 5. In this region, the horizontal dimension x correlates with particle energy E, illustrating a linear increase in energy in the $-x$ direction. This transformation projects the CeC Dogleg YAG image onto the $\{y, E\}$ plane, effectively mapping the longitudinal phase space.

The visualization in Fig. 6 provides a detailed representation of the longitudinal phase space $\{E, z\}$. Notably, the energy phase space tails, located at the bunch head and tail, form a shaded area extending from approximately $x = 0$ to the plot's right end in Fig. 5(b). Furthermore, the plot's turning points and plateau regions correlate directly with the bright areas on the left and right in Fig. 5(b), enhancing our understanding of the energy distribution within the beam.

This comprehensive approach to benchmarking using both transverse and longitudinal diagnostics significantly enhances our confidence in the simulation's fidelity and provides valuable insights into optimizing the CeC's operational parameters.

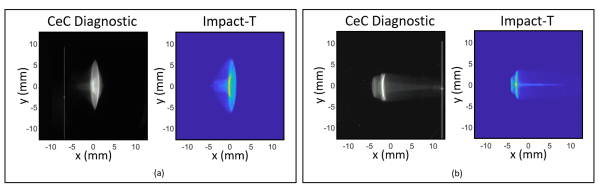

Figure 5: Comparison of CeC Dogleg YAG images against results from the Impact-T start-to-end simulation model. Images (a) and (b) represent beam profiles under different CeC lattice configurations.

CONCLUSION

In conclusion, the simulation accurately captured both the overall beam projection size and the intricate beam energy structures across various CeC lattice configurations. These results further validate the precision of our Impact-T start-to-end simulation model. Using this comprehensive model, our team successfully predicted the existence of a new plasma instability, which we have named Plasma Cascade Instability [12]. This discovery prevents the CeC electron beam from reaching saturation during transportation in the low-energy section and introduces a novel mechanism for density signal amplification in the interaction section. Moreover, this rigorously benchmarked model has significantly accelerated our design process for beam dynamics and machine tuning.

As we move forward, the next phase involves employing the Impact-T model for machine learning model training while the CeC accelerator undergoes servicing and development. We are confident that this well-validated simulation model will pave a clear path for our team toward achieving the objectives of the CeC demonstration.

REFERENCES

[1] Impact-Lbl, *Impact-LBL/impact-T: For impact-T beam dynamics code users and developers*. https://github.com/impact-lbl/IMPACT-T

[2] J. Qiang, S. Lidia, R. D. Ryne, and C. Limborg-Deprey, "Three-dimensional quasistatic model for high brightness beam dynamics simulation," *Phys. Rev. ST Accel. Beams*, vol. 9, p. 044 204, 2006. doi:10.1103/PhysRevSTAB.9.044204

[3] V. N. Litvinenko and Y. S. Derbenev, "Coherent electron cooling," *Phys. Rev. Lett.*, vol. 102, p. 114 801, 2009. doi:10.1103/PhysRevLett.102.114801

ISBN: 978-3-95450-247-9 ISSN: 2673-5490 doi: 10.18429/JACoW-IPAC2024-THPC06

[4] C. K. Birdsall and A. B. Langdon, *Plasma physics via computer simulation*. CRC press, 2018.

[5] I. Petrushina *et al.*, "High-brightness continuous-wave electron beams from superconducting radio-frequency photoemission gun," *Phys. Rev. Lett.*, vol. 124, p. 244 801, 2020. doi:10.1103/PhysRevLett.124.244801

[6] I. Petrushina *et al.*, "Measurements of the Electrical Axes of the CeC PoP RF Cavities," in *Proc. IPAC'19*, Melbourne, Australia, May 2019, pp. 3031–3034. doi:10.18429/JACoW-IPAC2019-WEPRB094

[7] J. Qiang, "A fast parallel 3d poisson solver with longitudinal periodic and transverse open boundary conditions for space-charge simulations," *Computer Physics Communications*, vol. 219, pp. 255–260, 2017. doi:10.1016/j.cpc.2017.06.002

[8] S. A. Belomestnykh *et al.*, "Commissioning of the 112 MHz SRF Gun and 500 MHz Bunching Cavities for the CeC PoP Linac," in *Proc. IPAC'15*, Richmond, VA, USA, May 2015, pp. 3597–3599. doi:10.18429/JACoW-IPAC2015-WEPWI049

[9] J. C. Brutus *et al.*, "Update on the CeC POP 704 MHz 5-Cell Cavity Cryomodule Design and Fabrication," in *Proc. IPAC'15*, Richmond, VA, USA, May 2015, pp. 3603–3605. doi:10.18429/JACoW-IPAC2015-WEPWI051

[10] B. Aune *et al.*, "Superconducting TESLA cavities," *Phys. Rev. ST Accel. Beams*, vol. 3, p. 092 001, 2000. doi:10.1103/PhysRevSTAB.3.092001

[11] P. Schauer and J. Bok, "Study of spatial resolution of yag:ce cathodoluminescent imaging screens," *Nuclear Instruments and Methods in Physics Research Section B: Beam Interactions with Materials and Atoms*, vol. 308, pp. 68–73, 2013. doi:10.1016/j.nimb.2013.05.006

[12] V. N. Litvinenko *et al.*, "Plasma-cascade instability," *Phys. Rev. Accel. Beams*, vol. 24, p. 014 402, 2021. doi:10.1103/PhysRevAccelBeams.24.014402